Electron Transfer Tunneling Pathways in Bovine Heart Cytochrome *c* Oxidase

Dmitry M. Medvedev, Iraj Daizadeh,† and Alexei A. Stuchebrukhov*

Contribution from the Department of Chemistry, University of California, Davis, California 95616, and Department of Molecular and Cellular Biology, Harvard University, Cambridge, Massachusetts 02138

Received January 5, 2000

Abstract: Results of a study of internal electron transfer in bovine heart cytochrome *c* oxidase with the method of tunneling currents are presented. Electronic structure of the protein complex is treated at the semiempirical extended Hückel level. Two distinct pathways connecting Cu_A and heme *a* are found, one of them is similar to proposed earlier in the literature, the other is new. The pathway connecting heme *a* and heme a_3 is also identified. This pathway differs from those proposed before. The calculated reaction rates between Cu_A and Fe_a and between Fe_a and Fe_{a3} are in reasonable agreement with experimental data. The tunneling matrix element for electron transfer from Cu_A to the binuclear site is found to be very small, which is consistent with experimental evidence of the absence of this reaction. With the assumption that evolution places constraints on functionally important amino acids, we suggest that amino acids implicated in the electron-transfer pathways will show a high degree of conservation in different organisms. Sequence analysis performed on subunit I and II revealed that this is indeed the case; amino acids of the identified tunneling pathways showed very little evolutionary variability.

1. Introduction

Cytochrome *c* oxidase (C*c*O) is the terminal membrane enzyme in the respiratory electron transport chain in mitochondria and many bacteria. It catalyzes the reduction of molecular oxygen to water supplying it with electrons obtained from cytochrome *c* on the outer side of the membrane and with protons from the inner side of the membrane. The reduction of each oxygen molecule is accompanied by the transfer of four additional protons across the membrane, from the inner side to the outer side. Electron and proton transfers are coupled to each other. Thus, C*c*O functions as a proton pump, which creates the proton gradient across the biological membrane at the expense of free energy of the redox reactions. Recent success in solving the structure of the enzyme has open the way for a detailed understanding of the mechanism of this molecular machine, which is one of the key components of biological energy conversion.

In this paper we study electron-transfer pathways between redox cofactors of C*c*O. The pathways are controlled by the structure of the protein. Understanding of electron transport chain is the first step toward the elucidation of the mechanism of function of this enzyme.

The bovine heart cytochrome *c* oxidase consists of 13 subunits.[1] It contains three redox cofactors: Cu_A, heme *a*, and the so-called binuclear site, which is the catalytic site of oxygen reduction. In addition to the redox centers, the enzyme contains sodium, magnesium, and zinc atoms.[2] Electrons from cytochrome *c* travel to the Cu_A site, then to heme *a*, and after that to the binuclear center via another heme located in the binuclear center.

The Cu_A site is located in the second largest subunit II. It consists of two copper atoms and six ligands: two cysteines, two histidines, a methionine, and a peptide carbonyl of a glutamate.[3] Two copper atoms are bridged by two cysteine sulfurs, and these four atoms are in the same plane. In addition, each copper atom is coordinated by an imidazole nitrogen of a histidine. The other two (axial) ligands are weak and do not play significant role in the electronic structure of the Cu_A site.[4−6] The structure of the Cu_A center without axial ligands is shown in Figure 1.

Both heme *a* and the binuclear site are located in the subunit I, the largest subunit. Low-spin heme *a* is coordinated by two imidazoles of histidine residues. It's propionates are directed toward the outer side of the membrane. The structure of heme *a* is shown in Figure 2. The binuclear site consists of another heme and another copper atom, called Cu_B. It's heme, called heme a_3, is a high-spin heme in the fully oxidized state of C*c*O, and is coordinated by only one imidazole of a histidine, while the copper atom is on the other side of the porphyrin plane. It is coordinated by three imidazoles of histidine ligands, leaving space between itself and the iron atom. This space is the binding site of oxygen molecule.[2] The structure of the binuclear site is shown in Figure 3.

* Address correspondence to this author.
† Harvard University.

(1) Tsukihara, T.; Aoyama, H.; Yamashita, E.; Tomizaki, T.; Yamaguchi, H.; Shinzawa-Itoh, K.; Nakashima, R.; Yaono, R.; Yoshikawa, S. *Science* **1996**, *272*, 1136.

(2) Yoshikawa, S.; Shinzawa-Itoh, K.; Nakashima, R.; Yaono, R.; Yamashita, E.; Inoue, N.; Yao, M.; Fei, M. J.; Peters Libeu, C.; Mizushima, T.; Yamaguchi, H.; Tomizaki, T.; Tsukihara, T. *Science* **1998**, *280*, 1723.

(3) Tsukihara, T.; Aoyama, H.; Yamashita, E.; Tomizaki, T.; Yamaguchi, H.; Shinzawa-Itoh, K.; Nakashima, R.; Yaono, R.; Yoshikawa, S. *Science* **1995**, *269*, 1069.

(4) Salgado, J.; Warmerdam, G.; Bubacco, L.; Canters, G. *Biochemistry* **1998**, *37*, 7378.

(5) Regan, J. J.; Ramirez, B. E.; Winkler, J. R.; Gray, H. B.; Malmström, B. G. *J. Bioenerg. Biomembr.* **1998**, *30*, 35.

(6) Gamelin, D. R.; Randall, D. W.; Hay, M. T.; Houser, R. P.; Mulder, T. C.; Canters, G. W.; de Vries, S.; Tolman, W. B.; Lu, Y.; Solomon, E. I. *J. Am. Chem. Soc.* **1998**, *120*, 5246.

10.1021/ja0000706 CCC: $19.00
Published on Web 06/30/2000

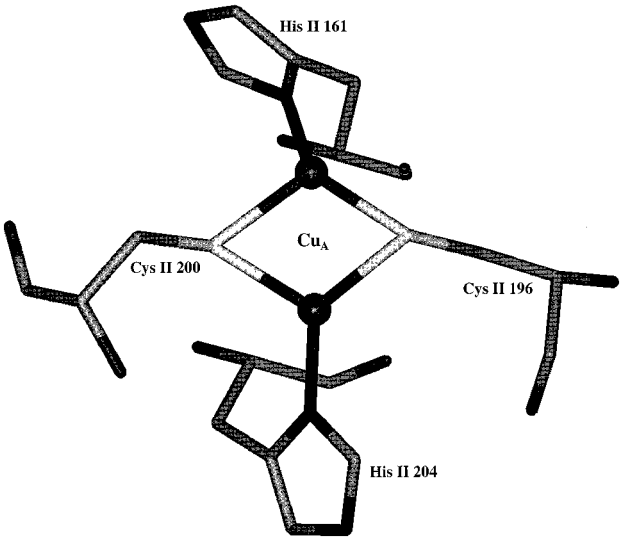

Figure 1. Structure of the Cu_A center without axial ligands and without hydrogen atoms. Cu atoms are marked with balls.

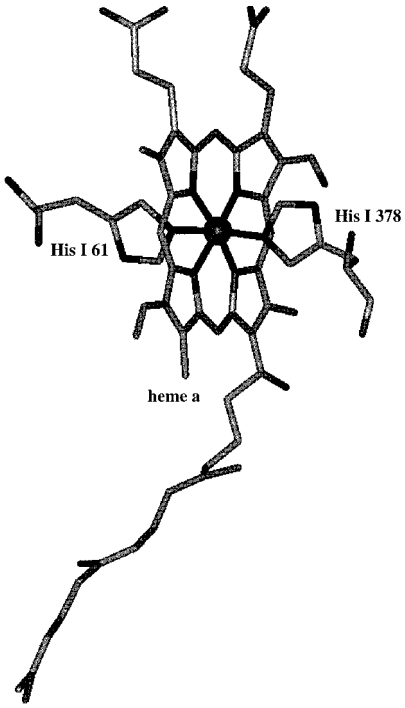

Figure 2. Structure of heme *a* without hydrogen atoms. Fe atom is marked with a ball.

It is known that electron transport chain runs from cytochrome *c* to Cu_A, then to heme *a*, and after that, via the iron atom of heme a_3, to the binuclear site. Thus, the reactions are as follows:

$$(2Cu)_A^{2+} + Fe_a^{3+} \rightarrow (2Cu)_A^{3+} + Fe_a^{2+}$$

and

$$Fe_a^{2+} + Fe_{a_3}^{3+} \rightarrow Fe_a^{3+} + Fe_{a_3}^{2+}$$

The charges indicated above are formal charges; real distribution of partial charges of atoms can differ significantly (see Results). Since electron transfer does not involve spin−orbital interaction, the total spin of the system is conserved.

Electron transfer (ET) between each pair of redox centers can be described by nonadiabatic electron transfer theory,[7] which

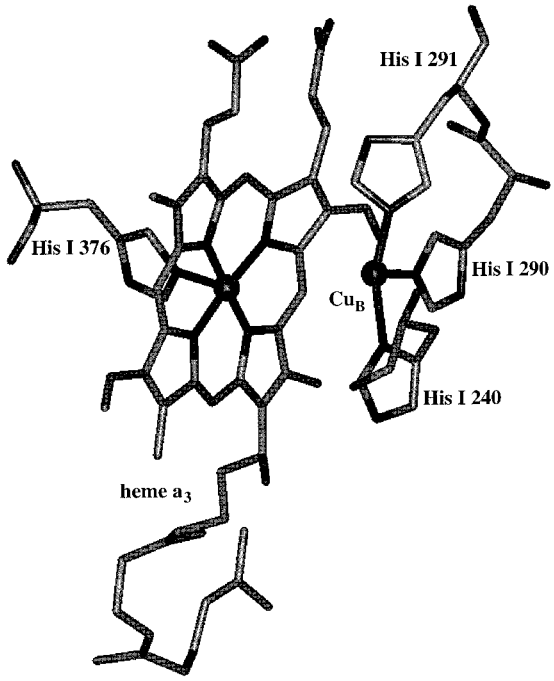

Figure 3. Structure of the binuclear site without hydrogen atoms. Fe and Cu atoms are marked with balls.

predicts that the rate of transfer (in classical approximation for nuclear vibrations) is

$$k = \frac{2\pi}{\hbar} \frac{|T_{DA}|^2}{\sqrt{4\pi\lambda k_B T}} \exp\left(-\frac{(\lambda + \Delta G^\circ)^2}{4\lambda k_B T}\right) \qquad (1)$$

Here T_{DA} is the tunneling matrix element (electronic coupling), k_B is the Boltzmann constant, λ is the Marcus reorganization energy, and ΔG° is the free energy, or the driving force, of the reaction. In this contribution we are interested in identifying tunneling pathways of electron transfer and evaluation of the tunneling matrix element T_{DA} for different ET reactions in C*c*O. The pathway analysis will be performed with the method of tunneling currents. Electronic structure of donor and acceptor complexes as well as of intervening medium will be treated within the extended Hückel approximation. Since C*c*O is a vital component of energy conversion processes in all evolutionarily diverse aerobic organisms, one can argue that possible evolutionary constraints were placed on the amino acids that are critical for the proper functioning of this enzyme. In particular, some constraints could be placed on the amino acids involved in the electron transport processes. To test this hypothesis, we performed database searches using as a query the primary sequences of subunits I and II of the bovine C*c*O to find biological homologues, and checked evolutionary stability of amino acids found in our pathway analysis. We find that both subunits I and II are ubiquitous in nature and are well-represented in at least two of three urkingdoms, which implies that this enzyme has existed in almost unchanged form since, at least, the prokaryotic/eukaryotic divergence, ca. 2 billion years ago.[8] Although it is difficult to distinguish between conserved amino acids critical for structural stability and those important for other potential functions, we find that most of the amino acids found in our pathway analysis are conserved evolutionarily.

(7) Marcus, R. A.; Sutin, N. *Biochim. Biophys. Acta* **1985**, *811*, 265.
(8) Nealson, K. H.; Conrad, P. G. *Philos. Trans. R. Soc. London B* **1999**, *354*, 1923.

2. Previous Work on the Subject

Pathways of internal electron transfer in cytochrome *c* oxidase have already been discussed in the literature.[5,6,9] Two pathways for the Cu_A−heme *a* electron transfer were proposed. One of them starts with $N^{\delta 1}$ of His^{204} of subunit II and proceeds through Arg^{438} and Arg^{439} of subunit I to the ring A propionate of the heme *a*.[5,10] The other starts with sulfur of Cys^{196} of subunit II and then proceeds through Tyr^{440} of subunit I and the already mentioned Arg^{438} and Arg^{439} of subunit I to the ring A propionate of the heme *a*.[6] Similar pathways were proposed for the cytochrome *c* oxidase from *Paraccocus denitrificans*,[9−11] whose core part (subunits I, II, and III) is almost identical to that of the mitochondrial C*c*O.[12]

For the heme *a*−heme a_3 electron-transfer three possible pathways were proposed.[5] They all start on His^{378} (ligand of the heme *a*) and finish on His^{376} (ligand of heme a_3), and differ in amino acids they use as intermediates. One of them uses Phe^{377} as the only intermediate and two others proceed through Val^{374} and Ala^{375}. The second pathways goes directly to His^{376} from Ala^{375}, while the third goes to Tyr^{372} first and then to His^{376} (all amino acids are in subunit I).

Pathways of the hypothetical Cu_A−heme a_3 electron transfer were also proposed,[5] but the estimated rate of reaction was very low, which is consistent with absence of experimental evidence of such transfer. Finally, attempts have been made to estimate the reorganization energy associated with these reactions.

The works mentioned above used the crystallographic structure obtained with 2.8 Å[1,3] resolution and did not treat the tunneling process in a rigorous quantum mechanical way. The method used for the analysis of the pathways accounted for only the structure of the system ignoring quantum interference effects.[5,6,10] In the present work we use improved crystallographic data obtained with 2.3 Å[2] resolution and treat the tunneling process with the method of tunneling currents. Electronic structure of the system is treated here within the extended Hückel approximation, and all details of the wave function of the whole complex are taken into account.

3. Methods

3.1. Crystallographic Data. In the calculations we used the crystallographic data of the fully oxidized (resting) bovine heart cytochrome *c* oxidase with 2.3 Å resolution.[2] For comparison, the calculations were also performed on the structure obtained with 2.8 Å resolution.[1,3] The coordinates were obtained from the Brookhaven Protein Database. Only subunits I and II, containing redox cofactors, were used in the calculations. Since the initial file with crystallographic coordinates did not contain hydrogen atoms, they were added to the system using simulation program Biograph.[13] It should be noted that in addition to hydrogen atoms the initial file did not contain phospholipids present in the system[1] and, what is especially important, did not contain water molecules. Therefore, water molecules, which can contribute to electron transfer, were not taken into account in our calculations.

The copper atom of the binuclear site is located at the distance of about 5 Å from the iron atom (depending on the oxidation state of the complex and it's ligands[2]) and is about 1 Å away from the normal to the heme plane going through the iron atom. The distance between Cu_A (the geometrical center of Cu_2S_2 complex, to be exact) and Fe_a is 20.7 Å, the distance between Cu_A and Fe_{a3} is 23.1 Å, and the distance between Cu_A and Cu_B is 22.5 Å. The distance between Fe_a and Fe_{a3} is 13.2 Å, and the edge-to-edge distance between two hemes is about 5 Å.

3.2. Extended Hückel Setting. In these calculations we used the method of tunneling currents in the framework of the extended Hückel approximation.[14] In this approximation, the states of valence electrons are represented in a basis of Slater-type atomic orbitals

$$\phi = Nr^{n-1}e^{-\zeta r} Z_{lm} \tag{2}$$

Here *n* is the main quantum number, ζ, the Slater exponent, Z_{lm}, the angular part for a given angular momentum *l*, which is a linear combination of spherical functions Y_{lm}, *N*, the normalization constant, and *r*, the distance from the nucleus. The above single-ζ approximation was used for all atoms except those of transition metals, for which the double-ζ Slater-type orbitals were used:

$$\phi = Nr^{n-1}(C_1e^{-\zeta_1 r} + C_2e^{-\zeta_2 r}) Z_{lm} \tag{3}$$

The diagonal elements of the Hamiltonian matrix are the empirical valence shell ionization potentials. The nondiagonal matrix elements are given by the Wolfsberg−Helmholtz expression:

$$H_{ij} = KS_{ij}\frac{H_{ii} + H_{jj}}{2} \tag{4}$$

with $K = 1.75$, where S_{ij} is the overlap of atomic orbitals *i* and *j*. Most of the parameters (Slater exponents and ionization potentials) were taken from parametrization of Alvarez.[15] Parameters for iron and sulfur atoms were obtained elsewhere.[16,17] The ionization potentials of d-orbitals of copper atoms and of p-orbitals of sulfur atoms in the Cu_A complex, that is, sulfurs of Cys^{196} and Cys^{200}, were chosen in such a way that the resulting wave function of Cu_A complex and corresponding electron density distribution (see Section 4) are qualitatively similar to those found in previous theoretical and experimental studies.[4,6,18,19] The resulting extended Hückel parameters are listed in Table 1.

3.3. Method of Tunneling Currents. The method of tunneling currents has been already described in the literature,[20−22] and therefore we will only briefly outline it here. Let $|pi\rangle$ be a basis set of atomic orbitals, which are not necessarily orthogonal to one another. Here *p* refers is the number of atom, and *i* is the number of orbital on this atom. These orbitals are assumed to be real, and so are all the matrix elements and coefficients of expansion of the wave function. Let $H_{pi,qj}$ be the Hamiltonian matrix of the system and $S_{pi,qj} = \langle pi|qj\rangle$ be the overlap matrix.

Let c^D_{pi} and c^A_{qj} be the coefficients of expansion of the donor $|D\rangle$ and acceptor $|A\rangle$ wave functions in terms of the atomic orbitals. The matrix of interatomic currents is defined by[21,22]

$$J_{pq} = \sum_{i\in p}\sum_{j\in q} J_{pi,qj} = \frac{1}{\hbar}\sum_{i\in p}\sum_{j\in q}(H_{pi,qj} - ES_{pi,qj})(c^D_{pi}\, c^A_{qj} - c^A_{pi}\, c^D_{qj}) \tag{5}$$

Here states $|D\rangle$ and $|A\rangle$ are localized donor and acceptor states (later referred to as simply donor and acceptor states), *E* is the tunneling energy, which is equal to the expectation value $\langle D|\hat{H}|D\rangle = \langle A|\hat{H}|A\rangle$ in

(9) Williams, K. R.; Gamelin, D. R.; LaCroix, L. B.; Houser, R. P.; Tolman, W. B.; Mulder, T. C.; de Vries, S.; Hedman, B.; Hodgson, K. O.; Solomon, E. I. *J. Am. Chem. Soc.* **1997**, *119*, 613.
(10) Ramirez, B. E.; Malmström, B. G.; Winkler, J. R.; Gray, H. B. *Proc. Natl. Acad. Sci. U.S.A.* **1995**, *92*, 11949.
(11) Iwata, S.; Ostermeier, C.; Ludwig, B.; Michel, H. *Nature* **1995**, *376*, 660.
(12) Michel, H.; Behr, A.; Harrenga, A.; Kannt, A. *Annu. Rev. Biophys. Biomol. Struct.* **1998**, *27*, 329.
(13) *Biograph*, ver. 3.22, The Molecular Design and Analysis Program; Molecular Simulations Inc.: San Diego, CA, 1992.
(14) Yates, K. *Hückel Molecular Orbital Theory*; Academic Press: New York, 1978.
(15) Alvarez, S. *Tables of Parameters for Extended Hückel Calculations*; Universitat de Barcelona: Barcelona, Spain, December, 1995.
(16) Tatsumi, K.; Hoffmann, R. *J. Am. Chem. Soc.* **1981**, *103*, 3328.
(17) Schilling, B. E. R.; Hoffman, R. *J. Am. Chem. Soc.* **1979**, *101*, 3456.
(18) Karpefors, M.; Slutter, C. E.; Fee, J. A.; Aasa, R.; Källebring, B.; Larsson, S.; Vänngård, T. *Biophys. J.* **1996**, *71*, 2823.
(19) Bertini, I.; Bren, K. L.; Clemente, A.; Fee, J. A.; Gray, H. B.; Luchinat, C.; Malmström, B. G.; Richards, J. H.; Sanders, D.; Slutter, C. E. *J. Am. Chem. Soc.* **1996**, *118*, 11658.
(20) Stuchebrukhov, A. A. *J. Chem. Phys.* **1996**, *104*, 8424.
(21) Stuchebrukhov, A. A. *J. Chem. Phys.* **1996**, *105*, 10819.
(22) Stuchebrukhov, A. A. *J. Chem. Phys.* **1997**, *107*, 6495.

Table 1. Parameters for Extended Hückel Calculation[a]

	shell	H_{ii}		ζ		ζ_1	ζ_2
atom	n	s	p	d	s	p	d	d
H	1	−13.6	−	−	1.3	−	−	−
C	2	−21.4	−11.4	−	1.625	1.625	−	−
N	2	−26.0	−13.4	−	1.950	1.950	−	−
O	2	−32.3	−14.8	−	2.275	2.275	−	−
Na	3	−5.1	−3.0	−	0.733	0.733	−	−
Mg	3	−9.0	−4.5	−	1.100	1.100	−	−
S[b]	3	−20.0	−13.3	−	1.817	1.817	−	−
	3	−	−12.0	−	−	1.817	−	−
Fe[c]	4	−8.39	−4.74	−	1.900	1.900	−	−
	3	−	−	−11.46	−	−	5.35 (0.5366)	1.80 (0.6678)
Cu	4	−11.4	−6.06	−	2.2	2.2	−	−
	3	−	−	−13.0	−	−	2.30 (0.57442)	5.95 (0.59332)

[a] Valence shell ionization potentials (H_{ii}) are in eV, Slater exponents (ζ) in au ζ_1 and ζ_2 are Slater exponents for double-ζ type orbitals of transition metals. Coefficients of corresponding single-ζ orbitals are given in parentheses. [b] Data are from ref 17, while ionization potential of p-orbitals of sulfur atoms of Cys[196] and Cys[200] of subunit II was taken to be equal to −12.0 eV (see Subsection 3.2). [c] Data are from ref 16; all other parameters, except for the ionization potential of d-orbitals of Cu atoms (see Subsection 3.2), are from ref 15.

the transition state, and $\hat{H}$ is the electronic Hamiltonian operator in the transition state.

When there is no resonance, states $|D\rangle$ and $|A\rangle$ can be approximated by two corresponding eigenstates of the entire system. These two eigenstates are identified by projecting all eigenstates of the system onto zeroth-order donor and acceptor states $|d\rangle$ and $|a\rangle$, which are obtained by diagonalization of the isolated donor and acceptor complexes, respectively. The donor and acceptor complexes are predefined sets of atoms, on which the states $|D\rangle$ and $|A\rangle$ are likely to be localized. Usually, the overlap of only one of the eigenstates of the entire system with zeroth-order state $|d\rangle$ or $|a\rangle$ is close to unity, while all other eigenstates have nearly zero overlaps. The interaction of the zeroth-order donor and acceptor states with the protein environment results only in their slight delocalization. However, this delocalization causes the effective interaction between the donor and acceptor states.

The magnitude of interatomic current J_{pq} is proportional to probability that the tunneling electron, once on atom q, will jump on to atom p during the tunneling transition from donor to acceptor. The total current through an atom p, that is, the sum of all positive currents J_{pq} flowing through p

$$N_p = \sum_q J_{pq}\theta(J_{pq}) \tag{6}$$

is proportional to the probability that electron will pass through atom p during the tunneling jump from donor to acceptor.[20−23] The value of N_p can be used to map all atoms in the protein that are involved in the electron transfer process. The interatomic currents provide quantitative information on the intensity and directionality of electron flow in the tunneling transition, and as such provide a quantitative description of what is commonly called tunneling pathways.

Let the system be divided into two parts by some closed surface, a dividing surface, so that the donor site and part of the bridge are inside one of the parts, and the acceptor site and the other part of the bridge are inside the other part. Then the following formula holds:[20,22]

$$T_{\mathrm{DA}} = \hbar \sum_{p\in S_{\mathrm{D}}} \sum_{q\notin S_{\mathrm{D}}} J_{pq} \tag{7}$$

Here S_{D} is the part of the system bounded by the dividing surface and containing the donor site. Thus, interatomic currents provide information not only about the tunneling pathways but also about the magnitude of electronic coupling. In the calculations, several types of dividing surfaces were used: a sphere surrounding the donor site, a sphere surrounding acceptor site, or a plain perpendicular to a straight line between them. The matrix element was evaluated by the above formula.

3.4. Pruning Procedure. The evaluation of expression of the tunneling matrix element requires exact diagonalization of the Hamiltonian matrix of the system. This is not possible for very large systems, such as cytochrome *c* oxidase. To truncate the system, leaving only those amino acids that are important for the electron transfer, the pruning procedure was used.[24]

For the pruning procedure an approximate expression for the tunneling matrix element obtained with perturbation theory is used[25,26]

$$T_{\mathrm{DA}} = \sum_{\alpha,\beta} (H_{a\alpha} - ES_{a\alpha})(ES^B - H^B)^{-1}_{\alpha\beta}(H_{\beta d} - ES_{\beta d}) \tag{8}$$

Here the sum is taken over all orbitals of the bridge, subscripts d and a refer to zeroth-order donor and acceptor states $|d\rangle$ and $|a\rangle$, and the superscript B shows that only bridge Hamiltonian and overlap matrixes are involved. Since they are usually sparse, evaluation of this sum can be made effectively without explicit evaluation of the inverse matrix by the method of transition amplitudes.[27]

The pruning procedure runs as follows. First, the perturbation matrix element of the whole system is evaluated, as described above. Then the truncation of the system is performed. We draw a line between donor and acceptor complexes, put spheres with given radius and centers on the line (spacing between centers is $R/20$, where R is the distance between geometrical centers of donor and acceptor complexes) and remove all the amino acids which do not have atoms inside these spheres. The dangling bonds created by this procedure are "repaired" by adding hydrogen atoms on the places of atoms whose bonds with kept atoms are cut. We repeat this procedure for a number of different values of truncation radius (values from 2 to 18 Å were used in the calculations presented) and find the value for which saturation of the matrix element is achieved —the matrix element of the system truncated with this radius is virtually equal to the matrix element of the whole system and further increase of truncation radius changes it only very slightly.

Once the truncation is done, the following procedure, which is pruning per se, is carried out. A selected amino acid is deleted from the protein, and the matrix element for a modified protein is evaluated and compared with that of the intact protein, then the amino acid is returned back to protein. In the deletion the dangling bonds are "repaired" as in the truncation procedures. The procedure is repeated for all amino acids except those which have atoms belonging to donor or acceptor complexes. After such probing, the amino acids whose deletion does not affect tunneling matrix element are permanently removed, retaining only those amino acids for which the value of the quantity

(23) Cheung, M. S.; Daizadeh, I.; Stuchebrukhov, A. A.; Heelis, P. F. *Biophys. J.* **1999**, *76*, 1241.

(24) Gehlen, J. N.; Daizadeh, I.; Stuchebrukhov, A. A.; Marcus, R. A. *Inorg. Chem. Acta* **1996**, *243*, 271.

(25) Stuchebrukhov, A. A. *Chem. Phys. Lett*. **1997**, *265*, 643.

(26) Priyadarshy, S.; Skourtis, S. S.; Risser, S. M.; Beratan, D. M. *J. Chem. Phys.* **1996**, *104*, 9473.

(27) Daizadeh, I.; Gehlen, J.; Stuchebrukhov, A. *J. Chem. Phys*. **1997**, *106*, 5658.

$$P_a = \frac{|T'_{DA} - T_{DA}|}{|T_{DA}|} \quad (9)$$

is greater than some particular number (0.005 in most of the calculations presented here). Here T_{DA} is the matrix element for the truncated system (which is virtually equal to that of the whole system), and T'_{DA} is the matrix element for the truncated system without given amino acid. Clearly, amino acids which are important for the tunneling process should give larger values of P_a. The set of values of P_a is called in the present paper the amino acid tunneling spectrum. Using it, those amino acids which are not important for the electron transfer process are removed, and the system is reduced to a much smaller one, which is equivalent to the initial system in terms of electron transfer. The Hamiltonian of the pruned system can be directly diagonalized, and rigorous calculations using the method of tunneling currents can be performed at various levels of electronic structure description, including ab initio level.[28−30]

3.5. Sequence Analysis Study. The primary sequences of subunits I and II were obtained from the PDB entry of the recently crystallized bovine heart cytochrome *c* oxidase[2] (PDB entry 2OCC) and used as query sequences for the database search. The nonredundant, highly curated SWISSPROT[31] database was searched via the standard, heuristic Smith−Waterman, BLAST program;[32] the program default search parameters were used.[33] To ensure that the sequences retrieved from the search were indeed biologically related to those of the queries, that is, homologous, and not simply retrieved by chance, an *E*-value of less than 0.001 was used as the cutoff criterion. From this search, it was found that 128 sequences were homologues of the subunit I chain, and 215 sequences were homologous to the subunit II polypeptide.

The accession numbers enumerating these sequences were extracted from the BLAST output and a file compliant with the FASTA format which contained the full sequences was generated from these accession numbers using the SWISSPROT web-based service.[31,34] A multiple alignment using the CLUSTALW program[35] was then constructed from these FASTA formatted files; the program default parameters were used.[36] The multiple alignment was then searched for regions where amino acids implicated in the electron transfer pathways resided. Sequences which contained gaps in these regions, possibly due to partial sequencing, were removed. We were thus left with two multiple alignments, one for subunit I with 92 sequences and another for subunit II with 206 sequences.

From the initial set of 128 sequences from subunit I, 109 were eukaryotic sequences, 16 were bacterial sequences, and 3 were Archaean sequences. From the initial set of 215 sequences of subunit II, 204 were eukaryotic sequences and 11 were bacterial sequences. From the final 92 sequences obtained for subunit I, 77 were eukaryotic sequences, 13 were bacterial sequences, and 2 were archaen sequences. From the final 206 sequences obtained for subunit II, 196 were eukaryotic sequences and 10 were bacterial sequences.[37] For this final set of sequences the analysis of conservation of amino acids of tunneling pathways was performed.

4. Results

4.1. Cu_A−Heme *a* Electron Transfer. The calculation was performed on the structure obtained with 2.3 Å resolution. The extended Hückel parameters used are listed in Table 1.

4.1.1. Electronic Structure of the Donor Complex. It is known that after the electron transfer from Cu_A to heme *a*, the Cu_A center is left with a semioccupied molecular orbital with spin density equally distributed over both halves of the complex with large amount of spin density on coppers and sulfurs and small amount of spin density on histidine ligands.[18,19] In the extended Hückel approximation this orbital is doubly occupied in the reduced state of the Cu_A complex and serves as the zeroth-order donor state. The composition of the donor state was in our calculations as follows: 41.7% of spin density (Mulliken population) was on copper atoms (19.7% on the copper atom coordinated by His^{161} and 22% on the copper atom coordinated by His^{204}), 51.9% on sulfur atoms (23.8% on sulfur of Cys^{196} and 28.1% on sulfur of Cys^{200}), 0.076% on $N^{\delta 1}$ of His^{161} and 1% on $N^{\delta 1}$ of His^{204} (1.1% and 1.5% on imidazole rings accordingly). This is not in exact agreement with results of calculation performed earlier[6] on the structure obtained with 2.8 Å resolution, which show 71% of spin density on copper atoms and 25% on sulfur atoms. The energy of the donor state was −10.75 eV.

4.1.2. Electronic Structure of the Acceptor Complex. The zeroth-order acceptor state is the SOMO of acceptor complex which includes heme without its big hydrocarbon "tail" and two histidine ligands (assuming that the oxidation state of iron is +3 and that propionates of heme are negatively charged). It is composed mainly of t-orbitals of iron, which are not exactly degenerate in a nonperfect octahedral environment. It is the highest (in energy) of three such orbitals. The Mulliken population analysis of the acceptor state shows that 60.5% of spin density is on the iron atom and no other atom has population greater than 3%. The wave function is significantly delocalized over aromatic porphyrin rings (94% of acceptor electron density is localized on the heme) and has small amount of spin density on histidine ligands. The energy of this orbital was −10.76 eV, and the tunneling energy was −10.76 eV, too.

4.1.3. Two Pathways. The pathways of electron transfer from Cu_A to heme *a* found in the calculation are shown in Figure 4. The amino acid tunneling spectrum is shown in Figure 5. Not all of the amino acids left in the system as a result of pruning procedure are shown in Figure 4; some of the less important amino acids have been left out. The intensity of color of atoms is proportional to the total current passing through a given atom. Some atoms, for which total current is greater than twice the whole current in the system, are shown with maximum intensity. Two distinct pathways are found. One of them (His^{204} pathway) starts on copper atom and proceeds through His^{204} of subunit I and Arg^{439} of subunit II to propionates of heme *a*. The other

(28) Heifets, E. N.; Daizadeh, I.; Guo, J.; Stuchebrukhov, A. A. *J. Phys. Chem. A.* **1998**, *102*, 2847.

(29) Daizadeh, I.; Guo, J.; Stuchebrukhov, A. A. *J. Chem. Phys*. **1999**, *110*, 8865.

(30) Stuchebrukhov, A. A. *J. Chem. Phys*. **1998**, *108*, 8499.

(31) Bairoch, A.; Apweiler, R. *Nucleic Acids Res.* **1999**, *27*, 49. The web site for accessing the SwissProt database is http://www.expasy.ch/sprot.

(32) Altschul, S. F.; Madden, T. L.; Schäffer, A. A.; Zhang, J.; Zheng, Z.; Miller, W.; Lipman, D. J. *Nucleic Acids Res.* **1997**, *25*, 3389. The BLAST suite of programs is available from http://www.ncbi.nlm.nih.gov/BLAST.

(33) The BLASTp program was used with the following default settings: Matrix: BLOSUM62, Gap Penalties: Existence: 11, Extension: 1.

(34) Sequences for COX1 APIME (accession number: P20374; GI: 116963) and COX2 APILI (accession number: P20375; GI: 117004) were collected from National Center for Biotechnology Information's (NCBI) nonredundant database.

(35) Thompson, J. D.; Higgins, D. G.; Gibson, T. J. *Nucleic Acids Res*. **1994**, *22*, 4673. ClustalW WWW Service at the European Bioinformatics Institute http://www2.ebi.ac.uk/clustalw, Rodrigo Lopez, Services Programme.

(36) The default parameters were: KTUP = 1, window length = 0, topdiag = 1, pairgap = 0.05, matrix BLOSUM, gap-open = 10, endgaps = 10, gap-extension = 0.05, gap-distance = 0.05.

(37) The distribution of different types of species in the final set of sequences was as follows: for subunit I, 77 eukaryotic sequences (49 Metazoa, 12 Viridiplantae, 10 Fungi, 2 Rhodophyta, 2 Euglenoza, 1 Myxogastria, 1 Stramenopiles), 13 bacterial sequences (6 Proteobacteria, 4 Firmicutes, 2 Cyanobacteria, 1 Thermus/Deinococcus group), and 2 archaen sequences (1 Euryarchaeota, 1 Crenarchaeota); for subunit II, 196 eukaryotic sequences (157 Metazoa, 2 Alveolata, 3 Euglenozoa, 11 Viridiplantae, 2 Rhodophyta, 1 stramenopiles, 20 Fungi) and 10 bacterial sequences (4 Firmicutes, 3 Proteobacteria, 2 Cyanobacteria, 1 Thermus/Deinococcus group).

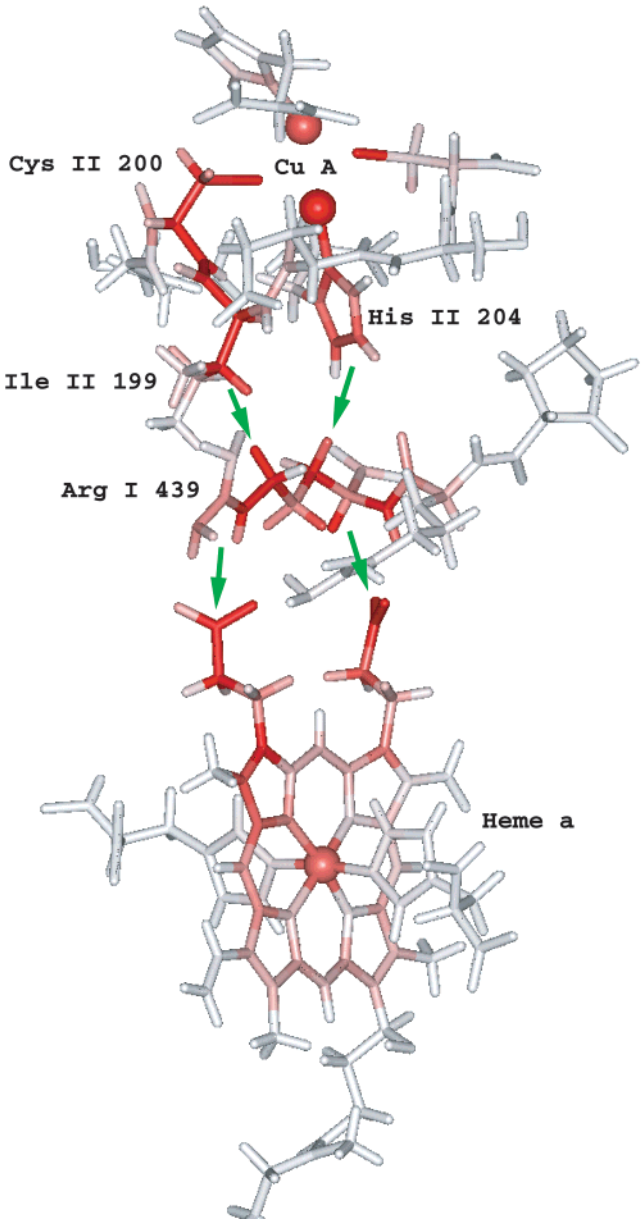

Figure 4. Pathways of electron transfer from Cu_A to heme *a*. Copper and iron atoms are marked with balls.

pathway (Cys^{200} pathway) starts with sulfur of Cys^{200} of subunit II and goes through Ile^{199} of subunit II and Arg^{439} of subunit I to the ring D propionate of heme *a*.

4.1.4. His^{204} Pathway. The His^{204} pathway is similar to the pathway described before,[5,10] but the current goes through Arg^{439} rather than Arg^{438}. It contains about 16 covalent bonds, one through-space jump, and one hydrogen bond. Due to delocalization of current it is impossible to identify the exact number of bonds comprising the pathway.

The through-space jump occurs between the His^{204} ring and the Arg^{439} of subunit I. It is delocalized and consists of two components: one is from $C^{\delta 2}$ of His^{204} to one of the β hydrogens of Arg^{439} (distance 3.5 Å) and the other is from $N^{\epsilon 2}$ of His^{204} to the same hydrogen of Arg^{439} (distance 3.3 Å). These two components have roughly the same intensity. Despite smaller distance between hydrogen on Arg^{439} and hydrogen bonded to $N^{\epsilon 2}$ of His^{204} (2.9 Å)) the current between them is 2.3 times smaller that the current between nitrogen itself and hydrogen on Arg^{439}. The current between $H^{\delta 2}$ of His^{204} and the hydrogen on Arg^{439} is much smaller. This can be explained by much greater amount of donor spin density on carbon and nitrogen than on histidine hydrogens.

The oxygen of Arg^{438} has been proposed to be the main acceptor of electrons from subunit II.[5,10] The distance between this oxygen and $N^{\epsilon 2}$ of His^{204} is almost the same as the distance between β hydrogen of Arg^{439} and $N^{\epsilon 2}$ of His^{204}, and the distance between this oxygen and $H^{\epsilon 2}$ of His^{204} is smaller than the distance between the β hydrogen of Arg^{439} and $H^{\epsilon 2}$ of His^{204} (2.5 and 2.9 Å respectively). The Mulliken population of both donor and acceptor states is greater on oxygen of Arg^{438} than on β hydrogen of Arg^{439}. Despite this we find that the current through this oxygen is smaller than that through the hydrogen (the ratio of total currents through these atoms is 1.8). This is explained by the smaller radius of oxygen atom, so that the overlaps between hydrogen orbitals and orbitals on atoms of histidine are greater than those between oxygen orbitals and orbitals on atoms of histidine, despite smaller or similar distance in the latter case (cf. Table 1). Actually the current through this oxygen is not only smaller than through β hydrogen of Arg^{439}, but also goes back to the donor complex. This is an example of the destructive quantum interference.

After the β CH_2 group of Arg^{439} the current is divided into three parts. One part returns to Cu_A center, another goes to the ring A propionate of heme *a* (this is the one which is adjacent to the $Arg^{438}-Arg^{439}$ peptide bond) and the other goes to the $NHC(NH_2)_2$ group of Arg^{439}. There it divides again, this time into two parts, one of which reaches the propionate mentioned above and the other eventually goes to the ring D propionate of heme *a*.

4.1.5. Cys^{200} Pathway. The Cys^{200} pathway was not identified before. It consists of about 16 covalent bonds (including the Fe−N bond in heme *a*, but excluding copper−sulfur bonds in Cu_A center), one hydrogen bond (from Arg^{439} to the ring D propionate of heme *a*), and one through-space jump from H^{β} of Ile^{199} of subunit II to H^{δ} of Arg^{439} of subunit I. The distance between these two hydrogen atoms is 1.9 Å. Also significant amount of current goes directly from C^{β} of Ile^{199} to H^{δ} of Arg^{439}.

We find that the Cys^{200} pathway is dominating, which is consistent with the large degree of delocalization of electron on sulfur of Cys^{200}. The ratio of currents going through Cys^{200} pathway to the current going through His^{204} pathway is about 3.5.

The current enters heme *a* through it's propionates. The ratio of current entering heme *a* through ring D propionate to the current entering heme *a* through the ring A propionate is about 4.1. Despite this the atom with maximal total current going through it is the carbon of the latter propionate. This is explained by the complicated system of circular current involving this propionate and a number of atoms of Arg^{438} and Arg^{439}.

4.1.6. Matrix Element. The value of matrix element is found to be 1.7×10^{-3} cm^{-1}. For the Cu_A−heme *a* electron-transfer reorganization energy was estimated to be equal to 0.3 eV,[38] which is unusually low for electron-transfer reactions in proteins. With $\lambda = 0.3$ eV the activationless reaction rate is 1.4×10^3 s^{-1}, which is about 10 times smaller than the rate observed in experiments.[38,39] In these experiments the rate was found to be $1-2 \times 10^4$ s^{-1}, depending on the oxidation state of heme a_3. With driving force of 90 *meV*[5] the rate constant calculated by Marcus' formula is 3.3×10^2 s^{-1}, and the matrix element calculated from experimental rate constant is about 1×10^{-2} cm^{-1}. One should keep in mind, however, that to estimate the

(38) Brzezinski, P. *Biochemistry* **1996**, *35*, 5611.
(39) Ädelroth, P.; Brzezinski, P.; Malmström, B. G. *Biochemistry* **1995**, *34*, 2844.

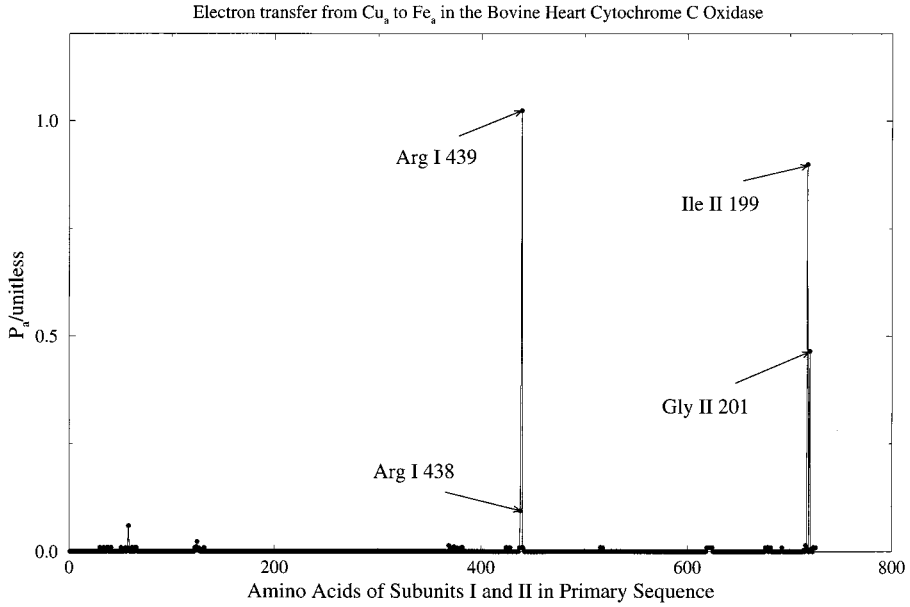

Figure 5. Amino acid tunneling spectrum of Cu_A-a electron transfer. Amino acids of subunit II are enumerated starting with number 520.

value of the reorganization energy from experimental data one needs either to know both temperature dependence of the rate and equilibrium constant (or, equivalently, the driving force of the reaction; cf. Marcus formula) or to have some information about the value of the tunneling matrix element. In the works sited above the temperature dependence of the rate of electron transfer from Cu_A to heme *a* was not determined, and it was assumed that the value of the tunneling matrix element depends exponentially upon distance between donor and acceptor: $T_{DA} = const \exp(-\beta(r - r_0))$, where β and r_0 were taken to be equal to 0.5 $Å^{-1}$ and 3.0 Å[38,39] respectively. The applicability of this approximation to the Cu_A-heme *a* electron transfer is not known, but for the hypothetical Cu_A-heme a_3 it gives results which do not agree with the results of pathway analysis (cf. subsection 4.3).

4.1.7. Sensitivity to Composition of Donor Wave function and to Protein Geometry. An additional calculation was performed with a second set of extended Hückel parameters in order to check the sensitivity of matrix element and tunneling pathways to details of donor wave function. The ionization potential of d-orbital of copper was changed from −13.0 to −12.3 eV. This changed the composition of the donor state. Now 59.6% of the spin density was localized on copper atoms (27.7% on the copper coordinated by His[161] and 31.9% on copper coordinated by His[204]); 28.8% was localized on sulfurs (12.5% on sulfur of Cys[196] and 16.3% on sulfur of Cys[200]), 4% on $N^{\delta 1}$ of His[161], and 3.8% on $N^{\delta 1}$ of His[204] (4.6 and 4.5% on imidazole rings, accordingly). This is more close to the results of calculations reported earlier, but the amount of spin density on histidine ligands seems to be overestimated[6] (in the calculations we refer to the total amount of spin density on NH_3 groups representing histidine ligands was only 3%). The asymmetrical charge distribution over copper atoms is consistent with these results, while asymmetrical distribution over sulfur atoms is not.

The acceptor wave function is almost identical to it's counterpart in the main calculation. Tunneling energy was equal to −10.65 eV.

The pathways found in this calculation are the same as in the previous one, but the His[204] pathway dominates in this case. Now 64% of the whole current is going through this pathway and 36% through Cys[200] pathway. This is consistent with the increased donor spin density on histidine ligands and decreased donor spin density on cysteine ligands.

The differences of the structure obtained as a result of pruning with the previous one are not significant. Some of the less important amino acids disappeared from the previous pruned molecule, and some new, also not really important, appeared in the new one. Tyr[440] and Ser[441] of subunit I were not removed specially to check the existence of proposed pathway through Tyr[440].

In comparison with the previous calculation the role of the δ CH group of His[204] and of oxygen of Arg[439] is greater. On the contrary, the role of the oxygen of Arg[438] is smaller. As a whole, the current through this oxygen goes back to subunit II, but it's amount is small, only only 3.5% of the whole current in the system (14% in the previous case). This is explained by the increased amount of spin density on the δ CH group of His[204] and decreased (relative to the δ CH group) spin density on the ϵ NH group of His[204].

Unlike the previous case, the current from sulfur of Cys[200] goes mainly not on the carbon covalently bonded with sulfur atom, but directly to NH group of cysteine. Eventually 39% of the current enters heme *a* through the ring D propionate and 61% through the ring A propionate.

The tunneling matrix element found in this calculation equals 1.75×10^{-3} cm^{-1}, which is very close to the result of the main calculation.

To check the sensitivity of our calculations to details of protein structure we performed calculations on the structure obtained with 2.8 Å resolution. The pathways were found to be the same. The most significant difference is that the current through Cys[200] pathway is now going back to the donor complex. Part of the current arriving on Arg[439] turns back and goes to the donor complex through the Cys[200] pathway. This turn also involves the ring D propionate of heme *a*, so that part of the current entering heme *a* through the ring A propionate leaves it through ring D propionate and goes back to the donor complex. Another difference is the increased role of oxygen of Arg[439], which is now the main acceptor of electrons from subunit II. It is explained by the reduction of distance between this oxygen and δ CH group of the imidazole ring of His[204] (the distance between oxygen of Arg[439] and $C^{\delta 2}$ is 3.2 Å in this

case and 3.4 Å in the structure obtained with 2.3 Å resolution). The value of matrix element was found to be 8.8×10^{-4} cm^{-1}. The decreased value of the matrix element is due to destructive interference in the Cys^{200} pathway.

4.1.8 Influence of the Protonation State of the Heme Propionates. Both propionates of heme *a* are deprotonated in our calculations. To explore influence of possible protonation, we performed several additional calculations. We added hydrogens to oxygens of propionates, one hydrogen at a time, trying all four oxygens. To add hydrogens we used programs Biograph[13] and xLEaP, the latter is a part of the simulation package AMBER 5.0.[40] We found that using these two programs results in different geometry of hydrogens bound to the same oxygen. This difference in geometry leads to noticeable difference in results since the current enters heme *a* through propionates. We performed eight calculations with added hydrogens (two calculations for each oxygen on propionates of heme *a*), and the calculated matrix element ranged from 1.1×10^{-3} to 4.1×10^{-3} cm^{-1}, though mainly staying between 1×10^{-3} and 2×10^{-3} cm^{-1}.

4.2. Heme *a*−Heme a_3 Electron Transfer. In the calculations for the heme *a*−heme a_3 electron transfer we chose the donor complex to be the same as the acceptor complex in the calculation for Cu_A−heme *a* electron transfer. The acceptor complex was chosen in the same way—all of the heme a_3 (except for it's hydrocarbon "tail") and the imidazole ring of the histidine ligand. The choice of the acceptor state is more complicated, however. It is known that Fe^{3+} is a high-spin ion when there is no ligand between heme a_3 and Cu_B and when there is a water molecule or a peroxide bound to the iron atom,[2,41] but is a low-spin ion when OH^- is bound to it.[5] Accordingly, the acceptor state should be different in these two cases. Since it is possible that during the catalytic cycle Fe_{a3} may accept electrons while being in its high-spin form, we performed calculations for both high-spin and low-spin heme a_3. To check possible influence of the sixth ligand of Fe_{a3} on tunneling pathways and value of tunneling matrix element calculations were performed both in the absence and in the presence of the peroxide ligand. It was found that the peroxide ligand does not change matrix element (it was changed not more than by a factor of 2) and tunneling pathways significantly, and, accordingly, results of calculations with it will not be presented here. We consider only tunneling pathways between heme *a* and heme a_3. We believe that these pathways do not depend on details of coupling between iron and copper atoms and that in any case electron enters the binuclear complex through the iron atom.

4.2.1. Calculations in the Case of High-Spin Heme a_3. For the study of electron transfer to a high-spin heme we chose as the zeroth-order acceptor state the lowest of those orbitals of the acceptor complex that consist mainly of t-orbitals of iron. In the absence of peroxide ligand 64.4% of electron density in the acceptor state was localized on the iron atom and 8.2% on His^{376}.

The donor state is almost identically the same as the acceptor state in the calculation for the Cu_A−heme *a* electron transfer, as it should be. Due to a short distance between the hemes direct overlap between zeroth-order donor and acceptor states is significant, and therefore direct current between the hemes is a large part of the overall current.

4.2.2. Tunneling Pathways in the Case of High-Spin Heme a_3. The pathways of electron transfer are shown in Figure 6, and amino acid tunneling spectrum in Figure 7. Atoms with total current greater of equal than the whole current in the system are shown with maximal intensity of color in Figure 6. Not surprisingly, only amino acids of subunit I were left after the pruning procedure.

Two pathways are found, and they are strongly coupled to each other. One of them is a direct jump from the methyl group of the ring D of heme *a* to it's counterpart on the ring D of heme a_3. The length of the jump is 3.4 Å between hydrogen on the methyl group of the ring D of heme *a* and hydrogen on the methyl group of the ring D of heme a_3 and 3.7 Å between the same hydrogen on heme *a* and carbon of the methyl group of the rind D of heme a_3.

The other pathway uses His^{378} and Phe^{377} as intermediates. Almost all current leaving the iron atom goes to the imidazole ring of His^{378}. Despite large individual currents between iron and atoms of heme *a*, their sum is only 2% of the whole current in the system, and there is a strong and very complicated system of circular currents in the porphyrin rings.

From the imidazole ring of His^{378} the current goes to the aromatic ring of Phe^{377}, mainly jumping directly from ϵ CH of His^{378} to ϵ1 CH of Phe^{377}. From the benzene ring of Phe^{377} the current goes to the ring D of heme a_3, to the methyl group on it, and to the α CH_2 of the ring D propionate of the heme. Significant amount of current also goes through bonds of His^{378} and Phe^{377} to β CH_2 group of Phe^{377}, from where it jumps to the ring D of heme a_3, mainly to the C2 carbon on this ring. The distance of this jump is 2.7 Å between this carbon and the β hydrogen of Phe^{377} and 3.3 Å between two carbons.

The current going from Phe^{377} to heme a_3 is about 88% of the whole current. Direct current from one heme to the other is about 23% of the whole current. The aromatic ring of Phe^{377} is involved in two complicated systems of circular currents—one includes ϵ1 CH and ζ carbon of Phe^{377} and the ring D of heme *a*, the other includes γ, δ1 and δ2 carbons and δ2 hydrogen of Phe^{377} and the ring D and α CH_2 group next to it on heme a_3. There is another complicated system of circular currents on the pyrrol rings of heme a_3 itself. In fact in both hemes there are currents from iron atom to heme atoms as well as from heme atoms to iron atom.

About 15% of the current goes back from heme a_3 to heme *a* via the side chain of Leu^{381}. Last, the current comes to His^{376} mainly not from Phe^{377} and not from heme a_3, but from Ala^{375}—it goes from His^{378} to Val^{374} via hydrogen bond between imidazole nitrogen and oxygen of Val^{374}, then through bonds to Ala^{375} and to His^{376}.

4.2.3. The Value of the Matrix Element. The tunneling energy was equal to −10.79 eV. The matrix element was calculated to be 0.39 cm^{-1}. The reorganization energy for this reaction was determined to be 0.76 eV,[39] and the driving force is about 40 meV.[39,42] Then the rate constant calculated by the Marcus' formula is 5.9×10^4 s^{-1}, while the experimental rate constant is about 2×10^5 cm^{-1}.[39,42] With this rate constant and given values of driving force and reorganization energy the value of matrix element should be about 0.7 cm^{-1}, which is only 1.8 times greater than the calculated value.

4.2.4. Calculations in the Case of Low-Spin Heme a_3. For the study of electron transfer to a low-spin heme we chose as the zeroth-order acceptor state the highest of those orbitals of acceptor complex that consist mainly of t-orbitals of iron, in

(40) Case, D. A.; Pearlman, D. A.; Caldwell, J. W.; Cheatham, T. E., III; Ross, W. S.; Simmeling, C. L.; Darden, T. A.; Merz, K. M.; Stanton, R. V.; Cheng, A. L.; Vincent, J. J.; Crowley, M.; Ferguson, D. M.; Radmer, R. J.; Seibel, G. L.; Singh, U. C.; Weiner, P. K.; Kollman, P. A. *AMBER 5*, University of California, San Francisco, 1997.

(41) Michel, H. *J. Am. Chem. Soc.* **1998**, *95*, 12819.

(42) Verkhovsky, M. I.; Morgan, J. E.; Wikström, M. *Biochemistry* **1992**, *31*, 11860.

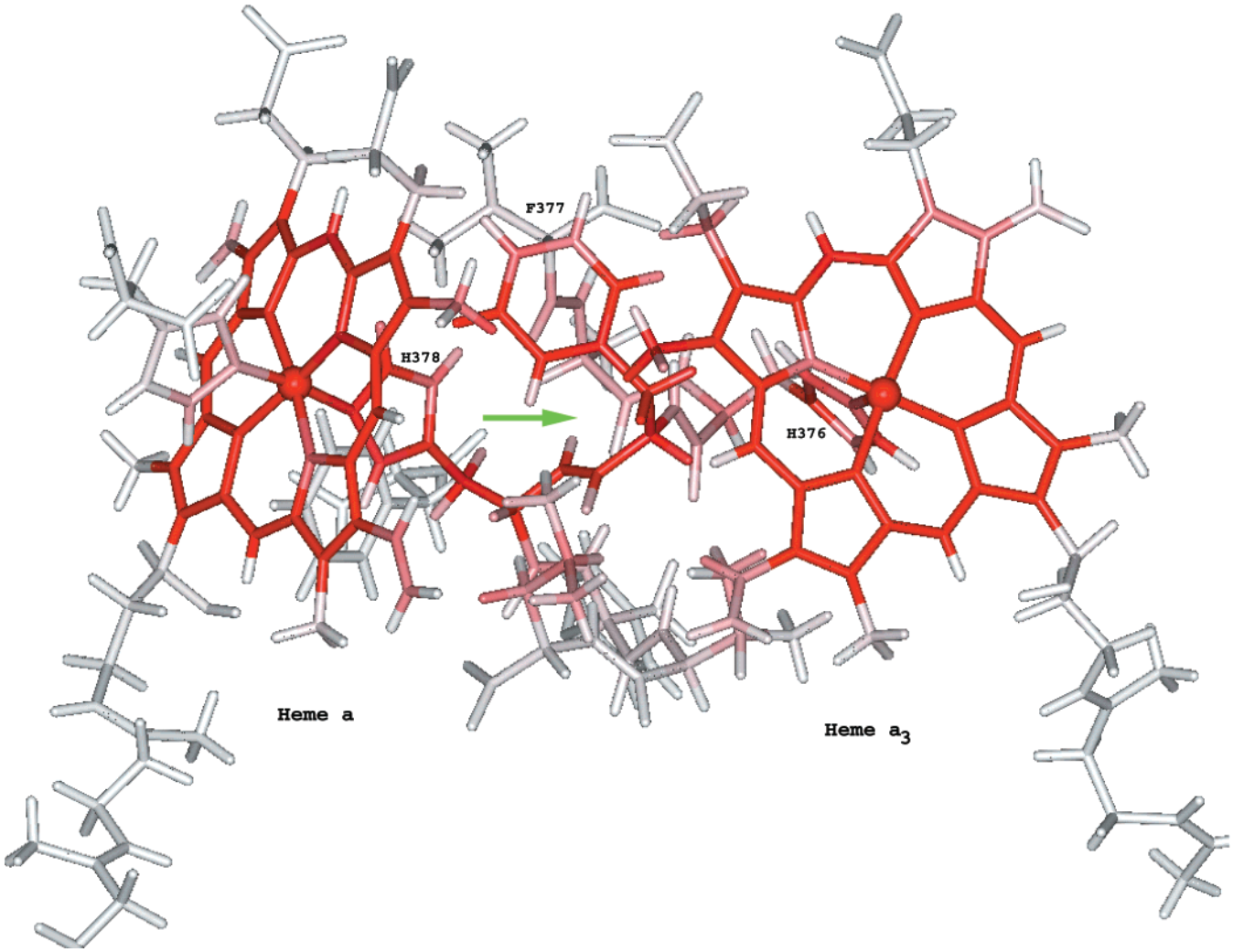

Figure 6. Pathways of electron transfer from heme *a* to heme a_3 in the case of high-spin heme a_3. Iron atoms are marked with balls.

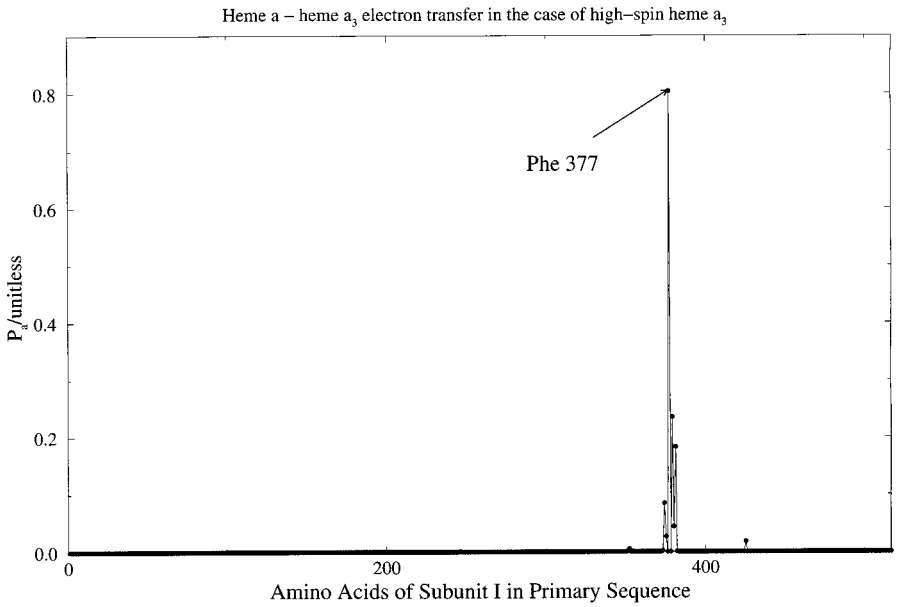

Figure 7. Amino acid tunneling spectrum of heme *a*−heme a_3 electron transfer in the case of high-spin heme a_3.

the same way as for the heme *a*. We found that it was the SOMO of acceptor complex (assuming that the oxidation state of iron is +3 and that propionates of heme a_3 are negatively charged), as it should be expected.

The donor state is the same as for the case of high-spin heme a_3. The acceptor state is more localized now—82% of spin density is localized on the iron atom, and no other atom has more than 2% of electron density on it.

The matrix element, calculated with tunneling energy −10.69 eV was equal to 0.43 cm^{-1}, which is very close to the previous case.

4.2.5. Tunneling Pathways in the Case of Low-Spin Heme a_3. There are significant differences between pathway pattern in the case of high-spin heme a_3 and that in the case of low-spin heme a_3. There are still two pathways, strongly coupled to each other. One of them is direct—the same as for the case of high-spin heme a_3. The other uses Phe^{377} as an intermediate. However, unlike the previous case, His^{378} and His^{376} do not play significant role. The current goes to the aromatic ring of Phe^{377} directly from heme *a* and from there to heme a_3. The importance of the two pathways is roughly the same: 57% of the whole current goes directly from one heme to the other, and 43% of the current goes through Phe^{377}.

As in the previous case, there are strong and complicated systems of circular currents, involving hemes and the aromatic ring of Phe^{377}. But unlike the previous case, residues other than hemes themselves and Phe^{377} do not play any significant role in the electron-transfer process.

4.2.6. Mutation of Phe^{377}. Mutation of Phe^{377} of subunit I of the ubiquinol oxidase from *Escherichia coli* to alanine leads to reduction of the rate of electron transfer from heme *o* to heme *b* approximately by a factor of 2: the time constant drops from 3−4 to 7−8 μs.[43] We have substituted Phe^{377} in the pruned molecule by an alanine and calculated matrix element. Substitution was made by two different programs: SCWRL[44] and Biograph.[13] Substitution by these two programs turned to lead to different geometries of the side chain of alanine amino acid, and hence to different values of matrix element. The value of matrix element was equal to 0.16 cm^{-1} (SCWRL) and 0.13 cm^{-1} (Biograph) in the case of high-spin heme a_3, and 0.3 cm^{-1} (both SCWRL and Biograph) in the case of low-spin heme a_3. This corresponds to reduction of rate by a factor of 5.9−9 in the case of high-spin heme a_3 and by a factor of approximately 2 in the case of low-spin heme a_3. The smaller change in rate in the latter case agrees with the observation that the greater part of the current goes directly from one heme to the other in that case.

The change in the rate found in our calculations (the change of which was greater than in the experiment) does not permit to make any definitive conclusions. First, our calculations were not performed on the cytochrome bo_3 from *E. coli*, the crystal structure of which is not known at present, but on bovine heart C*c*O. Second, the substitution of Phe^{377} performed as described above did not alter positions of hemes and other protein amino acids. It is likely, however, that upon replacement of bulky side chain of phenylalanine by a methyl group the edge-to-edge distance between two hemes will decrease, thus increasing direct electronic coupling between them.

4.3. Electron Transfer from Cu_A to the Binuclear Site. Experiments do not reveal any direct electron transfer from Cu_A to the binuclear site[1] despite similar distance from Cu_A to heme *a* and from Cu_A to heme a_3. We performed calculations for this hypothetical reaction. We made calculations of Cu_A−heme a_3 electron transfer, both for low-spin and high-spin heme (without the peroxide ligand), and of Cu_A−Cu_B transfer.

The calculated matrix element was 6.4×10^{-6} cm^{-1} for Cu_A−Cu_B transfer, 2.4×10^{-5} cm^{-1} for electron transfer from Cu_A to low-spin heme a_3, and 9.8×10^{-6} cm^{-1} for electron transfer from Cu_A to high-spin heme a_3. With the reorganization energy of 0.8 eV,[38] which is typical for electron transfer in proteins,[45] the highest of these values gives activationless reaction rate constant of 0.17 s^{-1}. This is several orders of magnitude smaller, than the rates of other electron-transfer reactions in the cytochrome *c* oxidase, which is consistent with absence of experimental evidence of this transfer.

One note should be made, however. Magnesium atom is coordinated by three water molecules,[2] which were absent in our calculations. Magnesium atom plays important role in the tunneling pathways from Cu_A to the binuclear site found in our calculations. These water molecules can play significant role in this hypothetical reaction and hence change the value of matrix element, though it is unlikely that it can become big enough to make this reaction competitive with other two.

4.4. Results of Sequences Analysis and Comparison with Previous Works. In this work two pathways are found for the Cu_A−heme *a* electron transfer. The His^{204} pathway is similar to the pathway described before,[5,10] but largely does not include Arg^{438} of subunit I. It is about two covalent bonds longer than the pathway proposed by Gray's group, which contains no through-space jumps but contains an additional hydrogen bond. The Cys^{200} pathway was not identified before. The His^{204} pathway consists of His^{204} of subunit II and Arg^{439} of subunit I, while the Cys^{200} pathway consists of Cys^{200} and Ile^{199} of subunit II and the same arginine. Pruning procedure showed that despite small amount of current going through it, Arg^{438} of subunit I is also important for electron transfer.

A pathway going through Cys^{196} of subunit II and Tyr^{440} of subunit I was proposed earlier.[6,9] We do not find this pathway. In fact, Tyr^{440} of subunit I does not even appear in the pruned molecule. This hypothetical pathway is about seven covalent bonds and one hydrogen bond longer, than the Cys^{200} pathway, but does not contain through-space jumps.

For the heme *a*−heme a_3 electron-transfer we found three major pathways. One of them is a direct jump between two hemes, another uses benzene ring of Phe^{377} as a sole intermediate, while the other uses imidazole ring of His^{378} and benzene ring of Phe^{377} as intermediates.

Three pathways of the heme *a*−heme a_3 electron transfer were proposed in the literature,[5] all starting and ending on iron atoms and going through His^{378} and His^{376}. One uses the part of backbone belonging to Phe^{377} and consists of 16 covalent bonds. The second pathway uses Val^{374} and Ala^{375} as intermediates between two ligating histidines, while the third uses Val^{374}, Ala^{375}, and Tyr^{372}. We do not find the third pathway; Tyr^{372} does not appear in the pruned molecule for all cases studied. As for the second pathway, our calculations show that there is some current going through it, but the magnitude of this current is small.

We have checked evolutionary stability of amino acids proposed to be important for electron transport. Results of this sequences analysis study are presented in Table 2. For Cu_A−heme *a* transition we find that all amino acids comprising the His^{204} pathway are well-conserved evolutionarily, with only Arg^{439} having three substitutions in 92 sequences studied. Arg^{438} is found to be totally conserved too. On the contrary, Ile^{199} of the Cys^{200} pathway is not conserved. However, possible absence of Cys^{200} pathway in other organisms does not seem to be important for the functioning of electron transport system, since there is a highly conserved His^{204} pathway, and due to it's high rate (of the order of 10^4 s^{-1}) Cu_A−heme *a* electron transfer is

(43) Verkhovsky, M. I. Private communication.

(44) Bower, M. J.; Cohen, F. E.; Dunbrack, R. L. *J. Mol. Biol.* **1997**, *267*, 1268.

(45) Gray, H. B.; Winkler, J. R. *Annu. Rev. Biochem.* **1996**, *65*, 537.

Table 2. Polymorphism of Amino Acids Relevant to the Various Electron Transfer Tunneling Mechanisms[a]

reaction	amino acid/ position	chain	num. of substitutions	% polymorphism
$Cu_A \rightarrow$ heme *a*	Cys/196	II	0	0.00
	Ile/199	II	29 [24L,1M,3T,1Y]	14.1
	Cys/200	II	0	0.00
	His/204	II	0	0.00
	Arg/438	I	0	0.00
	Arg/439	I	3 [1P, 2K]	3.26
	Tyr/440	I	38 [29I,3L,2M,4V]	41.3
heme *a* $\rightarrow$ heme a_3	Tyr/372	I	14 [14F]	15.2
	Val/374	I	3 [1G,2I]	3.26
	Ala/375	I	13 [10G,3R]	14.1
	His/376	I	0	0.00
	Phe/377	I	0	0.00
	His/378	I	0	0.00
	Leu/381	I	10 [6I,1M,1Q,2V]	10.9

[a] Subunit I has 92 sequences and subunit II has 206 sequences.

not a rate-limiting step in the turnover process. Finally, Tyr^{440} of subunit I, which was proposed by Solomon and co-workers[6] to participate in electron transfer, is highly polymorphic, in agreement with the results of our calculations which do not reveal the pathway going through it.

His^{378} and Phe^{377}, which are found to be important for the heme *a*−heme a_3 electron transfer, were found to be highly conserved evolutionarily. Of other amino acids, found only weakly participating in electron-transfer process, only Val^{374} shows low degree of polymorphism, while Ala^{375} and Leu^{381} are highly variable. Finally, of amino acids, which were proposed by Gray and co-workers[5] to participate in electron transfer but not found to be important in our pathway analysis, His^{376} is highly conserved (as it should be expected for a ligand of the iron atom), while Tyr^{372} is highly variable.

5. Conclusions

Calculations of tunneling pathways of internal electron transfer in cytochrome *c* oxidase were performed, using the semiempirical implementation of the method of tunneling currents. The crystallographic structure used in the calculations was obtained with higher resolution than that used in previous works on this subject. Compared with these works, not only structure of the system was taken into account, but the wave function of the whole system was treated in a more rigorous quantum-mechanical way. For a given structure the accuracy of the method of tunneling currents is limited only by the accuracy of electronic structure description, that is, by the accuracy of the extended Hückel approximation for the present case. The same method, however, can be used also with ab initio electronic structure calculations.[28−30,46]

Major pathways of Cu_A−heme *a* and of heme *a*−heme a_3 electron transfers were identified. For the latter transfer possibilities of both high-spin and low-spin heme a_3 were studied. Now that the general pathways are known, it is possible to perform ab initio calculations on truncated structures containing those residues which are important for the transfers.

Two main pathways (His^{204} pathway and Cys^{200} pathway) of Cu_A−heme *a* electron transfer were identified. Their relative importance depends on details of wave function and of geometrical structure of the system. Since they change in the course of molecular dynamics, it is likely that their relative importance is changing in time, so that on the average they both are important and one can speak only about average matrix element and general pathways. The pathway running through Cys^{196} of subunit II and Tyr^{440} of subunit I, proposed earlier, was not confirmed.

The calculated transfer matrix element for the Cu_A−heme *a* transition is too small to account for the observed rate of transfer. With $\lambda = 0.3$ eV and $\Delta G^\circ = 0.04$ eV the transfer matrix element calculated from the observed reaction rate would be about 1×10^{-2} cm^{-1}, that is, 6 times larger than in the calculations presented here, and even in the case of activation-less reaction (i.e., with $\lambda = 0.09$ eV) the matrix element is found to be 2−3 times larger. Possible reasons for this discrepancy include, along with insufficient accuracy of the extended Hückel approximation, the neglect of the influence of water molecules located inside the system. Both fixed and moving water molecules are likely to be contained in it. Water molecules located along the identified pathways may facilitate electron transfer and increase the tunneling matrix element. The study of water inside C*c*O and its possible influence on electron transfer is currently underway in this group. Another factor that can influence the rate of the transfer is the protonation state of residues involved in tunneling, such as propionates of heme *a*. It is possible that the changes of their protonation state can influence the value of the tunneling matrix element and therefore couple electron transfer to proton transfer.

Calculations were also performed for the case of possible direct electron transfer from Cu_A to the binuclear center. The calculated values of the matrix element proved to be very small, which is consistent with the absence of experimental evidence of such electron transfer.

There is a remarkable coincidence between amino acids that have been identified as important for the electron-transfer process and those from the results of the sequence analysis. If one assumes that constraints on amino acids were imposed by evolution to ensure an "optimal" electron transport, then conserved amino acids should point to possible candidates for electron-transfer pathways. The amino acids that contain the greatest amount of current flowing through them in our pathway analysis do demonstrate a high degree of conservation. Ile^{199} of subunit II is the only amino acid of those which were found important for electron transfer in our pathway analysis that does not show evolutionary conservation. However, the His^{204} pathway is highly conserved, so that at least one pathway for Cu_A−heme *a* electron transfer is present in all proteins considered in our sequence analysis. Our analysis cannot of course exclude the possibility that amino acids found to be conserved in the evolution of the enzyme are conserved because of their importance for protein stability or other possible biological functions rather than for electron transport. The evolutionary conservation of the pathways found in this paper, however, is intriguing.

Acknowledgment. We thank Dr. Jens Antony for help with file preparation, stimulating discussions of the material of the paper, and for his help with computer calculations. A.A.S. thanks M. Wikström and members of his research group for stimulating discussions. I.D. thanks Professor Walter Gilbert for encouragement and support during the period of this work, and Professor Charles Marshall for mentioning that position 196 in the GenBank sequence (GI:5921852) for COX2 PSEGY was

(46) Stuchebrukhov, A. A. *J. Chem. Phys.* **1998**, *108*, 8510.

incorrectly labeled as a Y when it should have been labeled as a C.

The work at Davis was supported by the research grant from the National Institutes of Health (GM54052-02) and by the fellowships to A.A.S. from the Sloan and Beckman Foundations. Computer support of JPL/Caltech Supercomputing Center is gratefully acknowledged.

JA0000706